Available online at www.sciencedirect.com
SCIENCE DIRECT
Journal of Photochemistry and Photobiology A: Chemistry 175 (2005) 79–88
Journal of Photochemistry and Photobiology A:Chemistry
www.elsevier.com/locate/jphotochem

Effects of DNA on driving force dependence of photoinduced electron transfer from the excited state of tris(2,2-bipyridine)ruthenium(II) to intercalators in DNA Distinction between intra- and inter-DNA pathways

Shunichi Fukuzumi *, Makiko Tanaka, Mari Nishimine, Kei Ohkubo

Department of Material and Life Science, Graduate School of Engineering, Osaka University, SORST, Japan Science and Technology Agency (JST), Suita, Osaka 565-0871, Japan

Received 17 January 2005; received in revised form 28 February 2005; accepted 16 March 2005
Available online 23 May 2005

Abstract

Photoinduced electron transfer (ET) dynamics from the excited state of a ruthenium complex [$Ru(bpy)_3^{2+}$ (bpy = 2,2′-bipyridine)] to a series of intercalators in DNA, 9-substituted-10-methylacridinium ions ($AcrR^+$, R = H, CH_2Ph, Pr^i and Ph), 3-substituted-1-methylquinolinium ions ($RQuH^+$, R = H, Me, CN and Br) and 4- and 5-methylphenanthridinium ions (4- and 5-$MePhen^+$), were examined from the emission decay profiles of $Ru(bpy)_3^{2+}$ in the absence and presence of DNA in an aqueous solution. Intercalation of $AcrH^+$ to DNA is found to result in inhibition of hydride transfer from an NADH model compound, 1-benzyl-1,4-dihydronicotinamide, to $AcrH^+$. In contrast, the rate constants of photoinduced ET of intercalated molecules to DNA become much larger than those of free intercalators in solution due to the positive shift in the one-electron reduction potentials by the intercalation into DNA. The *intramolecular* pathway of photoinduced ET from $Ru(bpy)_3^{2+*}$ bound electrostatically to DNA to intercalators bound to the same DNA molecule has been distinguished from the *intermolecular* pathway of photoinduced ET of intercalators bound to a different DNA molecule. The occurrence of photoinduced ET is examined by laser flash photolysis experiments which show the transient absorption spectra of the one-electron reduced intercalator when the ET is exergonic. The resulting data were analyzed in light of the Marcus theory of ET to determine reorganization energies of ET in DNA as well as in an aqueous solution.

Keywords: DNA; Electron transfer; Intercalation; Marcus theory; Reorganization energy

1. Introduction

Extensive studies have been devoted to elucidate the role of DNA double helix in mediating electron transfer between electron donors and acceptors bound to DNA by intercalation [1–12]. The question of how electrons travel through DNA is of fundamental importance in relation with development of DNA-inspired electronically active materials with self-organization properties [13–15]. The DNA double helix consists of a linear array of π-stacked, aromatic heterocyclic nucleobases within a polyanionic sugar-phosphates backbone, which provides an ideal medium of efficient electron transfer mediated by a π-stack [1–12]. Most studies have so far focused on distance dependence of electron coupling within the DNA duplex, since DNA may serve a novel medium to facilitate nonadiabatic long-range electron transfer, which leads to the oxidative damage of DNA [1–13]. However, the driving force of electron transfer of intercalators may also be changed by the presence of DNA, since the redox potential of an intercalated molecule may be altered by intercalation due to the change in the environment from an aqueous phase to a space between π-stacked nucleobase pairs. Only small changes in the redox potentials of intercalators in the presence of DNA have so far been reported in the pulse radiolysis studies [16]. In addition, the lack of appropriate intercalators having a wide

* Corresponding author. Tel.: +81 6 6879 7368; fax: +81 6 6879 7370.
E-mail address: fukuzumi@chem.eng.osaka-u.ac.jp (S. Fukuzumi).

1010-6030/$ – see front matter © 2005 Elsevier B.V. All rights reserved.
doi:10.1016/j.jphotochem.2005.03.026

range of redox potentials have precluded the detailed investigation of the effects of DNA on the driving force dependence of photoinduced electron transfer of intercalated molecules.

We report herein the systematic study on the effects of DNA medium on the driving force dependence of photoinduced electron transfer of a series of intercalators which have a wide redox potential range [17]. The system we have chosen is the combination of $Ru(bpy)_3^{2+}$ (bpy = 2,2′-bipyridine) with cationic π-molecules such as acridinium and quinolinium ions, which can intercalate into DNA [17]. Since $Ru(bpy)_3^{2+}$ binds only electrostatically with DNA [18–21], the change in the redox potentials of intercalators by the binding to DNA may be directly reflected to the change in the photoinduced electron transfer. The detailed analysis of emission decay dynamics of $Ru(bpy)_3^{2+}$ with the intercalators in the presence of DNA enables us to determine the photoinduced electron transfer rate constants (first-order) of groove binding ruthenium complexes with the nearest intercalated molecules and also the photoinduced electron transfer rate constants (second-order) of groove binding ruthenium complexes with free molecules in an aqueous solution separately. The driving force of both types of electron transfer have been determined by the electrochemical measurements of groove binding ruthenium complexes, intercalated molecules in DNA, and intercalators in an aqueous solution. The resulting data were evaluated in light of the Marcus theory of electron transfer [22–24] to determine the reorganization energies of both types of electron transfer.

2. Experimental section

2.1. Materials

Calf-thymus deoxyribonucleic acid, sodium salt (DNA) and tris(2,2′-bipyridine)ruthenium dichloride ($[Ru(bpy)_3]Cl_2$) were purchased from Sigma Chem. Co., USA. Stock solution of DNA (18 mg in 25 mL sol.) were prepared by dissolution overnight in 5 mM Tris–HCl buffer (pH 7.0) containing 5 mM sodium sulfate (Na_2SO_4). Tris(hydroxy-methyl)aminomethane was purchased from Nacalai Tesque, Japan. Hydrochloric acid and sodium sulfate (99.9%) were purchased from Wako Pure Chemical Ind. Ltd., Japan. 10-Methylacridinium iodide was prepared by the reaction of acridine with methyl iodide in acetone, and it was converted to the perchlorate salt ($AcrH^+ClO_4^-$) by addition of $Mg(ClO_4)_2$ to the iodide salt, and purified by recrystallization from methanol [25,26]. 9-Substituted 10-methylacridinium perchlorates ($AcrR^+ClO_4^-$: R = Pr^i, CH_2Ph and Ph) were prepared by the reaction of 10-methylacridone in dichloromethane with the corresponding Grignard reagents (RMgX), then addition of sodium hydroxide for the hydrolysis and perchloric acid for the neutralization, and purified by recrystallization from ethanol-di ethyl ether [27]. 4-Methyl- and 5-methylphenanthridinium iodides (4- and 5-$MePhen^+I^-$) were prepared by the reaction of the corresponding phenanthridines, obtained commercially, with methyl iodide in acetone and purified by recrystallization from EtOH. 1-Methylquinolinium perchlorate ($QuH^+ClO_4^-$), 3-bromoquinolinium perchlorate ($BrQuH^+ClO_4^-$), 3-cyanoquinolinium perchlorate ($CNQuH^+ClO_4^-$) 1,3-dimethyl quinolinium perchlorate ($MeQuH^+ClO_4^-$), were prepared by the reaction of the corresponding quinoline derivatives with methyl iodide in acetone, followed by the metathesis with magnesium perchlorate [27]. Purification of water (18.3 MΩ cm) was performed with a Milli-Q system (Millipore; Milli-RO 5 plus and -Q plus). Acetonitrile was purified and dried by the standard procedure [28].

2.2. Electrochemical measurements

Cyclic voltammetry measurements were performed at 298 K on a BAS 100 W electrochemical analyzer in deaerated Tris–HCl buffer containing 5 mM Na_2SO_4 as supporting electrolyte. A conventional three-electrode cell was used with a gold working electrode (surface area of 0.3 mm^2) and a platinum wire as the counter electrode. The gold working electrode (BAS) was routinely cleaned by soaking it in concentrated nitric acid, followed by repeating rinsing with water and acetone, drying at 353 K prior to use in order to avoid possible fouling of the electrode surface. The reference electrode was an Ag/0.01 M AgCl. The cyclic voltammograms were measured with various sweep rates in a deaerated solvent containing Na_2SO_4 (5 mM) at 298 K. The second harmonic ac voltammetry (SHACV) [29] measurements were performed on a BAS 100B electrochemical analyzer in deaerated 5 mM Tris–HCl buffer (pH 7.0) containing 5 mM Na_2SO_4 as a supporting electrolyte at 298 K to determine the one-electron oxidation and reduction potentials. The gold working electrode (BAS) was polished with BAS polishing alumina suspension and rinsed with acetone before use. The counter electrode was a platinum wire (BAS). The values (versus Ag/AgCl) are converted to those versus SCE by adding 0.04 V [30].

2.3. Spectroscopic measurements

All change in the UV–vis spectra of several substrates were monitored by using a Hewlett Packard 8453 diode-array spectrophotometer. The interaction between intercalators and DNA were examined from the change in the UV–vis spectra of intercalators in the presence of various concentrations of DNA (0–1.7×10^{-3} M). Concentration of DNA per nucleotide phosphate were determined by absorption spectroscopy using a molar extinction coefficient of 6600 M^{-1} cm^{-1} at 260 nm [31].

Time-resolved fluorescence spectra were measured by a Photon Technology International GL-3300 with a Photon Technology International GL-302, nitrogen laser/pumped dye laser system, equipped with a four channel digital delay/pulse generator (Stanford Research System Inc. DG535) and a motor driver (Photon Technology International

MD-5020). Excitation wavelength was 480 nm using coumarin 480 (Exciton Co., USA) as a laser dye.

For nanosecond laser flash photolysis experiments, deaerated 5 mM Tris–HCl buffer solutions (pH 7.0) of 4-MePhen$^+$ containing Ru(bpy)$_3^{2+}$ in the presence and absence DNA were excited by a Panther OPO pumped by Nd:YAG laser (Continuum, SLII-10, 4–6 ns fwhm) at $\lambda = 450$ nm with the power of 5 mJ per pulse. The photochemical reactions were monitored by continuous exposure to a Xe-lamp (150 W) as a probe light and a photomultiplier tube (Hamamatsu 2949) as a detector. The transient spectra were recorded using fresh solutions in each laser excitation. All experiments were performed at 298 K.

3. Results and discussion

3.1. Driving force of photoinduced electron transfer in the absence and presence of DNA

In order to evaluate the driving force of photoinduced electron transfer from the excited state of Ru(bpy)$_3^{2+}$ [(Ru(bpy)$_3^{2+*}$; * denotes the excited state] to intercalators, the one-electron redox potentials of Ru(bpy)$_3^{2+}$ and intercalators in the absence and presence of DNA were determined respectively. Intercalators employed in this study are shown in Fig. 1. The one-electron oxidation potential (E^0_{ox}) of Ru(bpy)$_3^{2+}$ at ground state in deaerated 5 mM Tris–HCl buffer aqueous solution is determined as 1.18 V versus SCE by the cyclic voltammetry (CV) and the E^0_{ox} value remains the same in the presence of DNA (1.3×10^{-3} M). The one-electron oxidation potential of Ru(bpy)$_3^{2+*}$ at excited state (E^{0*}_{ox}) was determined from E^0_{ox} and visible absorption and fluorescence spectra (vide infra). In contrast, the one-electron reduction potential of AcrH$^+$ determined by the second harmonic ac voltammetry (SHACV) measurements (see Section 2) is shifted to a positive direction in the presence of DNA as compared with the value in its absence. The potential shift value increases with increasing concentration of DNA to reach a constant value (+0.19 V) where the ratio of concentrations of DNA to AcrH$^+$ is larger than 20 as shown in Fig. 2a. In the case of AcrPr^{i+}, a reversible CV wave is observed for the one-electron redox couple of AcrPr^{i+}/AcrPr$^{i\cdot}$ at -0.70 V (versus SCE) in deaerated 5 mM Tris–HCl buffer aqueous solution and this is also shifted to a positive direction,

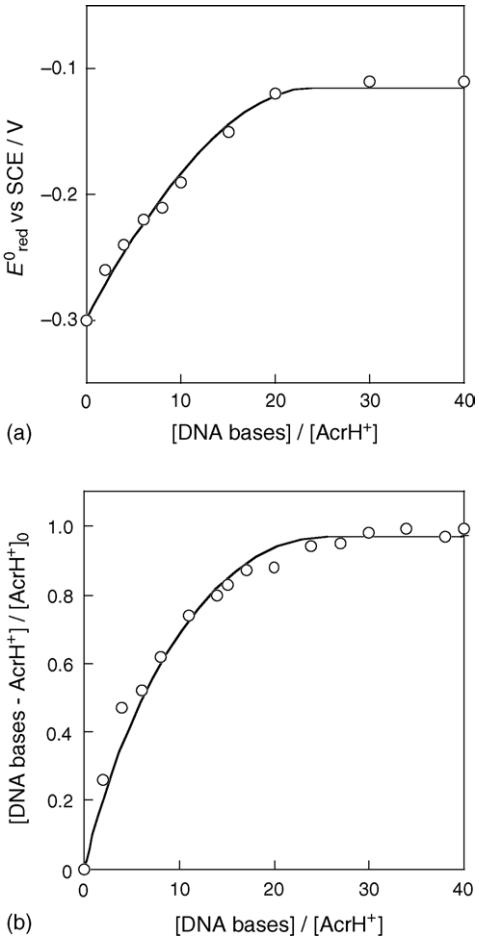

Fig. 2. (a) Plot of the one-electron reduction potential (E^0_{red}) of AcrH$^+$ (5.0×10^{-5} M) vs. concentration of DNA in a 5 mM Tris–HCl buffer aqueous solution (pH 7.0), determined by SHACV. (b) Plot of the ratio of intercalated AcrH$^+$ (5.0×10^{-5} M) vs. concentration of DNA in 5 mM Tris–HCl buffer (pH 7.0).

exhibiting a reversible wave at −0.56 V (versus SCE) [17]. Virtually the same results were obtained by the SHACV measurements. Similarly positive potential shifts are observed for other acridinium, quinolinium and phenathridinium ions as listed in Table 1. Such potential shifts in the presence of DNA may be attributed to the intercalation of these cationic species into DNA. Since only single reversible wave is observed irrespective of DNA concentration, the intercalated cation molecules in DNA are in equilibrium with free cation

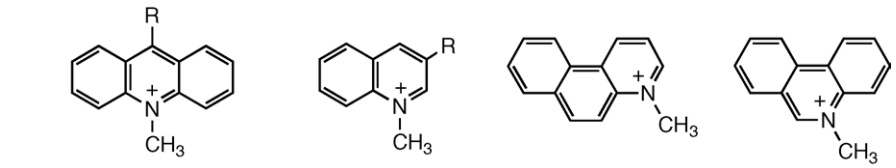

Fig. 1. Structures of intercalators in this study.

Table 1
One-electron reduction potentials of intercalators in the presence and absence of DNA, and driving forces and rate constants of photoinduced electron transfer (ET)

No.	Intercalator	E^0_{red} vs. SCE (V)[a]	Aqueous solution		Intermolecular ET (II)		Intermolecular ET (III)		Intramolecular ET (I)	
			$-\Delta G^\circ_{et}$ (eV)	k_{et} ($M^{-1}\,s^{-1}$)	$-\Delta G^\circ_{et}$ (eV)	k_{et} ($M^{-1}\,s^{-1}$)	$-\Delta G^\circ_{et}$ (eV)	k_{et} ($M^{-1}\,s^{-1}$)	$-\Delta G^\circ_{ET}$ (eV)	k_{ET} (s^{-1})
1	$AcrH^+$	−0.11 (−0.30)	0.59	6.5×10^9	0.59	2.2×10^9	0.78	2.8×10^9	0.78	3.0×10^7
2	$AcrCH_2Ph^+$	−0.45 (−0.48)	0.41	5.0×10^9	0.41	[b]	0.44	[b]	0.44	7.1×10^7
3	$AcrPr^{i+}$	−0.56 (−0.70)	0.19	4.8×10^9	0.19	[b]	0.33	[b]	0.33	4.5×10^7
4	$AcrPh^+$	−0.59 (−0.67)	0.22	3.1×10^9	0.22	[b]	0.30	[b]	0.30	4.8×10^7
5	$CNQuH^+$	−0.60 (−0.79)	0.10	1.4×10^9	0.10	6.9×10^8	0.29	2.6×10^9	0.29	4.0×10^7
6	$BrQuH^+$	−0.76 (−0.82)	0.07	8.6×10^8	0.07	5.2×10^8	0.13	2.3×10^9	0.13	1.0×10^7
7	5-$MePhen^+$	−0.78 (−0.87)	0.02	3.0×10^8	0.02	6.4×10^7	0.11	1.8×10^9	0.11	[c]
8	4-$MePhen^+$	−0.80 (−0.93)	−0.04	8.9×10^7	−0.04	5.7×10^7	0.09	1.6×10^9	0.09	[c]
9	QuH^+	−0.81 (−0.94)	−0.05	3.1×10^7	−0.05	6.7×10^7	0.08	4.4×10^9	0.08	[c]
10	$MeQuH^+$	−1.01 (−1.08)	−0.19	2.1×10^6	−0.19	1.0×10^7	−0.12	[c]	−0.12	[c]

[a] Values in parentheses are determined in 5 mM Tris/HCl (pH 7.0).
[b] The k_{et} values could not be determined accurately because of low solubility of intercalators.
[c] Too slow to be determined accurately.

molecules outside DNA at the time scale of CV and SHACV measurements.

A bathchromic shift and hypochromicity of its visible absorption band is observed in the electronic absorption spectrum of $AcrH^+$ in the presence of DNA in deaerated 5 mM Tris–HCl buffer as compared to that in the absence of DNA. From the absorbance change of $AcrH^+$ with DNA concentration is obtained the ratio of the intercalated $AcrH^+$ molecules by using Eq. (1)

$$\frac{[\text{DNA–AcrH}^+]}{[\text{AcrH}^+]_0} = \frac{A_0 - A}{A_0 - A_\infty} \tag{1}$$

where $[\text{DNA–AcrH}^+]$ and $[\text{AcrH}^+]_0$ are the concentrations of the intercalated $AcrH^+$ and the initial concentration of $AcrH^+$, and A_0, A, and A_∞ are the initial absorbance in the absence of DNA and that at a given concentration of DNA and at the large concentration of DNA when all $AcrH^+$ molecules intercalated into DNA, respectively. The $[\text{DNA–AcrH}^+]/[\text{AcrH}^+]_0$ value increases with increasing concentrations of DNA to reach unity where the ratio of concentrations of DNA to $AcrH^+$ is larger than 20 as shown in Fig. 2b. This value agrees with that observed for the potential shift in the presence of DNA (Fig. 2a). Such agreement confirms that the potential shift results from the intercalation of $AcrH^+$ to DNA.

Intercalation of $AcrH^+$ to DNA results in inhibition of hydride transfer from an NADH model compound, 1-benzyl-1,4-dihydronicotinamide (BNAH), since BNAH in an aqueous solution cannot interact with intercalated $AcrH^+$ embedded between base pairs in DNA (vide infra). Although hydride transfer from BNAH to $AcrH^+$ occurs efficiently in deaerated 5 mM Tris–HCl buffer (pH 7.0) at 298 K to yield 1-benzylnicotinamidinium ion (BNA^+) and 10-methyl-9,10-dihydroacridine ($AcrH_2$) [25,32], the hydride transfer is retarded significantly in the presence of DNA. Rates of hydride transfer were determined from the decrease in absorbance at 358 nm due to $AcrH^+$. The second-order plots for the rates of hydride transfer from BNAH to equivalent amount of $AcrH^+$ in the absence and presence of various concentrations of DNA gave straight lines (Fig. 3). From the slopes of linear plots of $1/([\text{AcrH}^+] - [\text{AcrH}^+]_\infty)$ versus time are obtained the second-order rate constants (k_{obs}) of the hydride transfer reaction. The k_{obs} value decreases with an increase in the ratio of $[\text{DNA bases}]_0/[\text{AcrH}^+]_0$. Such a retarding effect of DNA on the hydride transfer reaction indicates that the reactivity of $AcrH^+$ toward BNAH is diminished when $AcrH^+$ is intercalated to DNA. If one assumes that hydride transfer from BNAH occurs only to unbound $AcrH^+$ in solution as shown in Scheme 1, k_{obs} can be expressed as a function of [DNA] by Eq. (2),

$$k_{obs} = \frac{k^0_{obs}}{1 + K[\text{DNA}]} \tag{2}$$

where k^0_{obs} is the rate constant in the absence of DNA and K is the binding constant of $AcrH^+$ with DNA. From Eq. (2) is derived the ratio of the intercalated $AcrH^+$ molecules as

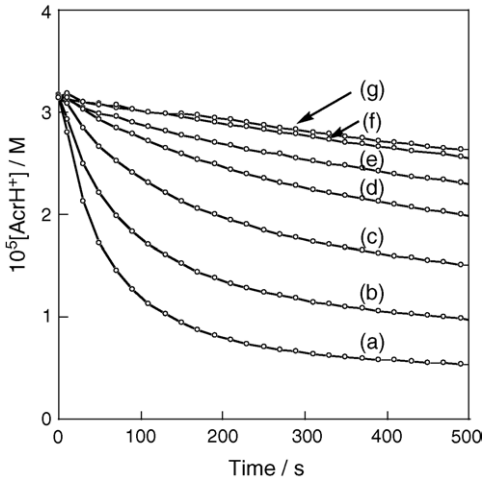

Fig. 3. Decay rate profiles of hydride transfer from BNAH (3.2×10^{-5} M) to AcrH$^+$ (3.2×10^{-5} M) in the absence and presence of various concentrations of DNA in 5 mM Tris–HCl buffer (pH 7.0) at 298 K; [DNA] = (a) 0, (b) 1.4×10^{-4}, (c) 2.8×10^{-4}, (d) 4.7×10^{-4}, (e) 7.1×10^{-4}, (f) 9.4×10^{-4} and (g) 1.4×10^{-3} M.

shown in Eq. (3).

$$\frac{[\text{DNA–AcrH}^+]}{[\text{AcrH}^+]_0} = \frac{k^0_{\text{obs}} - k_{\text{obs}}}{k^0_{\text{obs}}} \tag{3}$$

Plot of $(k^0_{\text{obs}} - k_{\text{obs}})/k^0_{\text{obs}}$ versus $[\text{DNA}]_0/[\text{AcrH}^+]_0$ is shown in Fig. 4, which agrees with the plot in Fig. 2. Such an agreement strongly indicates that AcrH$^+$ is intercalated to DNA and that BNAH cannot access to the intercalated AcrH$^+$ embedded between the nucleic acid base.

The driving force of the photoinduced electron transfer ($-\Delta G^\circ_{\text{et}}$) was determined by Eq. (4),

$$-\Delta G^\circ_{\text{et}} = e(E^0_{\text{red}} - E^{0*}_{\text{ox}}) \tag{4}$$

where E^0_{red} is the one-electron reduction potential of intercalators, the E^{0*}_{ox} is the one-electron oxidation potential of Ru(bpy)$_3^{2+*}$ and e is elementary charge. The E^{0*}_{ox} in deaerated 5 mM Tris–HCl buffer is determined as −0.89 V (versus SCE) from the E^0_{ox} value in the ground state (1.18 V versus SCE) and the free energy change between the ground and excited states (ΔG^* = 2.07 eV) [33–35]. Since the E^0_{ox} value is virtually the same irrespective of the absence or presence of DNA (vide supra), the effects of DNA on the driving force of electron transfer result from the positive shift of the E^0_{red}

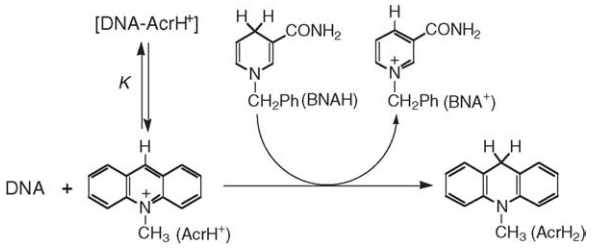

Scheme 1.

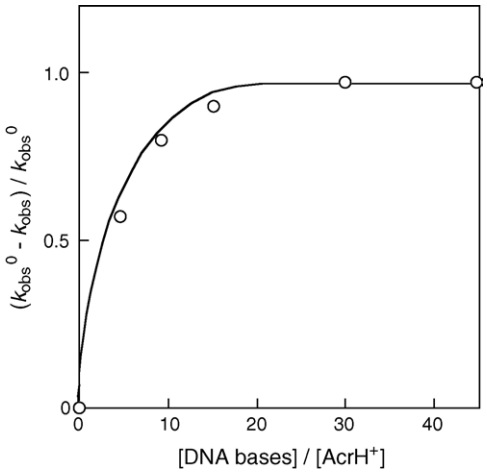

Fig. 4. Plot of $(k^0_{\text{obs}} - k_{\text{obs}})/k^0_{\text{obs}}$ vs. [DNA bases]/[AcrH$^+$] for hydride transfer from BNAH to AcrH$^+$ in the presence of various concentrations of DNA in 5 mM Tris–HCl buffer (pH 7.0) at 298 K.

values of intercalators in the presence of DNA. The driving forces of photoinduced electron transfer in the absence and presence of DNA are also listed in Table 1. The largest change in the driving force by the presence of DNA is obtained for AcrH$^+$ (0.19 eV) and CNQuH$^+$ (0.19 eV) whereas the smallest change is obtained for AcrCH$_2$Ph$^+$ (0.03 eV). This indicates the steric effect of the substituent plays an important role in the π–π interaction of the intercalator with base pairs of DNA and also in solvation with solvent molecules outside DNA. In any case, the photoinduced electron transfer from Ru(bpy)$_3^{2+*}$ to intercalators becomes more exergonic in the presence of DNA as compared with that in its absence.

3.2. Effects of DNA on rates of photoinduced electron transfer

First, the rate constants of photoinduced electron transfer from the excited state of Ru(bpy)$_3^{2+}$ to a series of intercalators in Table 1 were determined by the emission lifetime measurements of the excited states of Ru(bpy)$_3^{2+}$ used as an electron donor in the presence of intercalators in deaerated 5 mM Tris–HCl buffer (pH 7.0) at 298 K. The emission decay of Ru(bpy)$_3^{2+*}$ in the presence of each intercalator without DNA in Table 1 obeys first-order kinetics [36]. A typical example is shown in Fig. 5 for the photoinduced electron transfer (ET) from Ru(bpy)$_3^{2+*}$ to AcrH$^+$. The decay rate constant (k_d) increases linearly with increasing concentration of AcrH$^+$. The rate constant of *intermolecular* photoinduced ET (k_{et}) is determined from the slope of the linear plot of k_d versus concentration of AcrH$^+$. Similarly the k_{et} values of *intermolecular* photoinduced ET from Ru(bpy)$_3^{2+*}$ to a series of intercalators were determined as listed in Table 1. The occurrence of photoinduced electron transfer from Ru(bpy)$_3^{2+*}$ to intercalators was confirmed by the transient absorption spectra of the electron transfer products (e.g., AcrH$^\bullet$ at 520 nm) [37] as described in detail later.

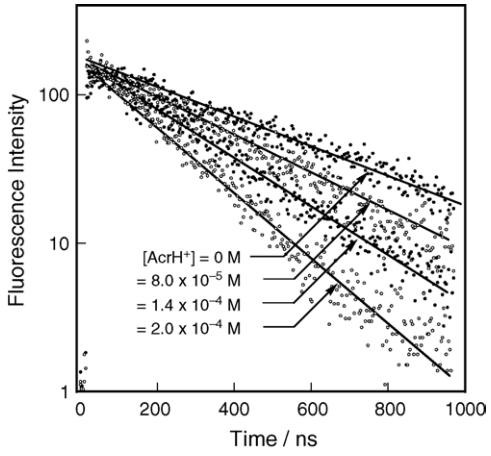

Fig. 5. Decay profile of emission of $Ru(bpy)_3^{2+*}$ in the presence of various concentrations of $AcrH^+$ in 5 mM Tris–HCl buffer (pH 7.0) at 298 K.

The driving force dependence of $\log k_{et}$ for photoinduced ET from $Ru(bpy)_3^{2+*}$ to a series of intercalators without DNA is shown in Fig. 6, exhibiting a typical feature of ET reactions: the $\log k_{et}$ value increases with increasing the driving force to reach a plateau value which corresponds to the diffusion rate constant ($8.0 \times 10^9\ M^{-1}\ s^{-1}$) [33] as the photoinduced electron transfer becomes energetically more favorable (i.e., more exergonic) [33].

According to the Marcus theory of electron transfer, the observed rate constant of *intermolecular* electron transfer is given as:

$$\frac{1}{k_{et}} = \frac{1}{k_{diff}} + \frac{1}{Z \exp[-(\lambda/4)(1 + \Delta G^{\circ}_{et}/\lambda)^2 / k_B T]} \quad (5)$$

where k_{diff} is the diffusion rate constant, Z is the collision frequency which is taken as $1 \times 10^{11}\ M^{-1}\ s^{-1}$, λ is the reorganization energy of electron transfer, k_B is the Boltzmann constant and T is the absolute temperature [22,38]. By fitting the data in Fig. 6 with the Marcus equation for bimolecular ET reactions Eq. (5), an experimental value of 0.60 eV is deduced for the reorganization of photoinduced ET from $Ru(bpy)_3^{2+*}$ to intercalators without DNA as shown by the solid line in Fig. 6.

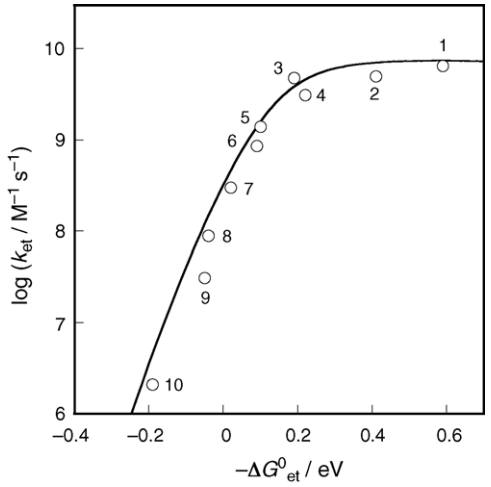

Fig. 6. Marcus plot of $\log k_{et}$ vs. $-\Delta G^{\circ}_{et}$ in 5 mM Tris–HCl buffer (pH 7.0). Numbers refer to intercalators in Table 1.

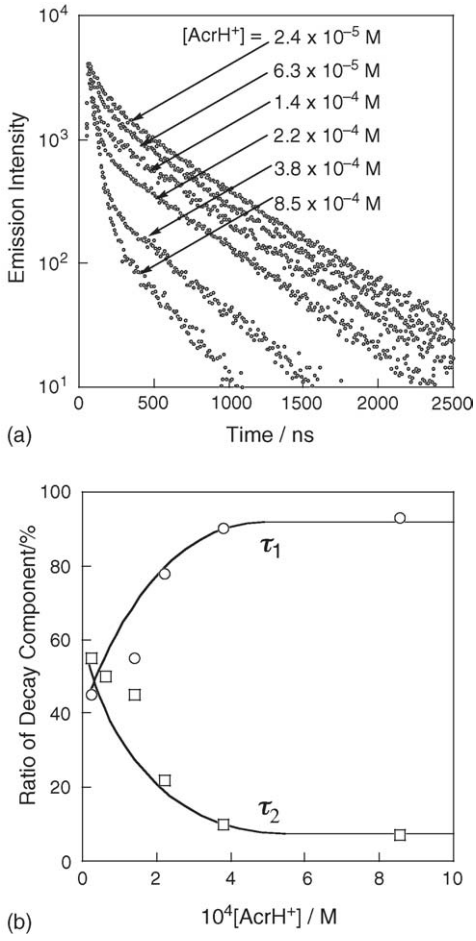

Fig. 7. (a) Emission decay profiles of $Ru(bpy)_3^{2+*}$ in the presence of $AcrH^+$ in deaerated 5 mM Tris–HCl buffer (pH 7.0) containing DNA (1.4×10^{-3} M) at 298 K observed by excitation at 490 nm. (b) Ratio of fluorescence decay components of $Ru(bpy)_3^{2+*}$ vs. concentration of $AcrH^+$.

In contrast to the clean single-exponential decay of the emission of $Ru(bpy)_3^{2+*}$ in the presence of $AcrH^+$ without DNA, the emission decay of $Ru(bpy)_3^{2+*}$ with $AcrH^+$ in the presence of DNA (1.4×10^{-3} M) can be well fitted with two exponentials as shown in Fig. 7a [39]. It should be noted that the emission decay of $Ru(bpy)_3^{2+*}$ in the presence of DNA without $AcrH^+$ obeys first-order kinetics with virtually the same lifetime as that in the absence of DNA. This indicates that $Ru(bpy)_3^{2+*}$ is not quenched by DNA. The lifetime of the faster component (τ_1) is constant irrespective of concentration of $AcrH^+$, whereas the slower component (τ_2) becomes faster with increasing concentration of $AcrH^+$. However, the percentage of the faster component increases with increasing concentration of $AcrH^+$ to reach 100%, whereas the slow component (τ_2) decreases to zero (Fig. 7b). If groove binding $Ru(bpy)_3^{2+}$ were free to migrate along the phosphate backbone of DNA to which $AcrH^+$ is intercalated, the emission

decay would be single-exponential. Thus, the two-exponential emission decay in Fig. 7 indicates that $Ru(bpy)_3^{2+*}$, bound electrostatically to DNA [18,19], is quenched by the nearest-neighbor $AcrH^+$ molecule, which is intercalated to the same DNA molecule as $Ru(bpy)_3^{2+}$. The distance dependence of the rate constant of *intramolecular* ET (k_{ET}) is given by Eq. (6),

$$k_{ET} = k_{ET}^{\circ} \exp(-\beta R) \quad (6)$$

where k_{ET}° is the rate constant of adiabatic *intramolecular* ET, R is the donor-acceptor center-to-center distance and β is dependent on the nature of the environment which affects the electronic coupling between the donor and acceptor molecules [40–43]. In DNA, the β value has been determined as 0.77 $Å^{-1}$ [42], when an increase in R by the DNA π-stacking distance (3.4 Å) results in a significant decrease in the k_{ET} value (1/14). The larger β value would lead to the larger decrease in the k_{ET} value. In such a case, Thus, the rate constant of *intramolecular* photoinduced ET (k_{ET}) from $Ru(bpy)_3^{2+*}$ to $AcrH^+$ in DNA is determined from the shorter lifetime ($k_{et} = \tau_1^{-1}$). Similarly the k_{ET} values of a series of 10-methylacridinium ion derivatives ($AcrCH_2Ph^+$, $AcrPr^{i+}$, $AcrPh^+$), 1-methylquinolinium ion derivatives ($CNQuH^+$ and $BrQuH^+$), phenthridinium ion derivatives (4-$MePhen^+$ and 5-$MePhen^+$) were determined as listed in Table 1, where k_{ET} and k_{ET} denotes the rate constants of *intramolecular* ET and *intermolecular* ET, respectively.

When intercalators which have lower E_{red}^0 value than $BrQuH^+$ are employed, the emission of $Ru(bpy)_3^{2+*}$ exhibits single-exponential decay even in the presence of DNA as shown in Fig. 8a for the emission quenching by 4-$MePhen^+$ in the presence of DNA (1.4×10^{-3} M). In this case, the first-order decay rate constant (k_d) increases significantly with increasing concentration of 4-$MePhen^+$ to reach a nearly constant value which increases with a smaller slope with a further increase in 4-$MePhen^+$ concentration as shown in Fig. 8b, where the magnitude of the initial increase in the k_d value increases with increasing DNA concentration. Such an accelerating effect of DNA may be ascribed to *intermolecular* photoinduced ET from $Ru(bpy)_3^{2+*}$ bound to DNA electrostatically to 4-$MePhen^+$ intercalated into a different DNA molecule from that bound to $Ru(bpy)_3^{2+}$. The concentration of 4-$MePhen^+$ intercalated into DNA [DNA bases-4-$MePhen^+$] is determined from the absorption change by intercalation. A plot of k_d versus [DNA bases–4-$MePhen^+$] affords a linear correlation as shown in Fig. 9.

From the slope is determined the k_{et} value of *intermolecular* photoinduced ET from $Ru(bpy)_3^{2+*}$ bound to DNA electrostatically to 4-$MePhen^+$ intercalated into a different DNA molecule from that bound to $Ru(bpy)_3^{2+}$ as 1.6×10^9 M^{-1} s^{-1}. This value is 28 times larger than the k_{et} value of *intermolecular* photoinduced ET from $Ru(bpy)_3^{2+*}$ bound to DNA electrostatically to free 4-$MePhen^+$ in solution (5.7×10^7 M^{-1} s^{-1}), determined from the smaller slope of the plot of k_d versus [4-$MePhen^+$] (Fig. 8b). The k_{et}

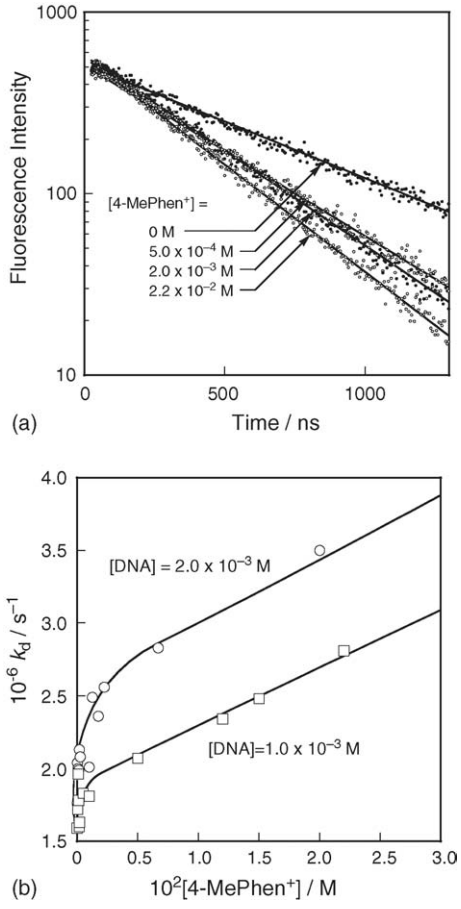

Fig. 8. (a) Emission decay profile of $Ru(bpy)_3^{2+*}$ in the presence of 4-$MePhen^+$ in deaerated 5 mM Tris–HCl buffer (pH 7.0) containing DNA (1.3×10^{-3} M) at 298 K observed by excitation at 490 nm. (b) Plots of k_d vs. [4-$MePhen^+$] in the presence of DNA (1.0×10^{-3} and 2.0×10^{-3} M) in deaerated 5 mM Tris–HCl buffer (pH 7.0).

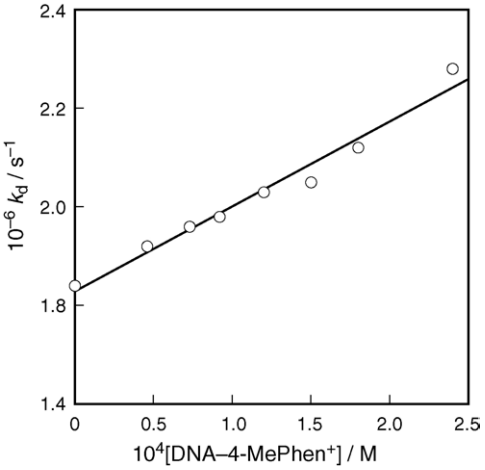

Fig. 9. Plot of k_d vs. concentration of intercalated 4-$MePhen^+$ [DNA bases–4-$MePhen^+$] for intermolecular photoinduced ET from $Ru(bpy)_3^{2+*}$ to 4-$MePhen^+$ in the presence of DNA (1.4×10^{-3} M) in deaerated 5 mM Tris–HCl (pH 7.0) at 298 K.

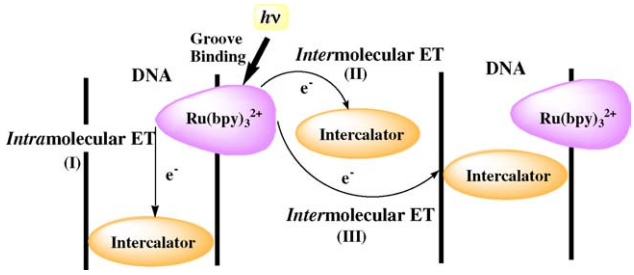

Scheme 2.

value of *intermolecular* photoinduced ET from $Ru(bpy)_3^{2+*}$, bound to DNA electrostatically, to free 4-MePhen$^+$ is virtually the same as the value in the absence of DNA ($8.9 \times 10^7\ M^{-1}\ s^{-1}$).

As shown above, there are three types of photoinduced ET from $Ru(bpy)_3^{2+*}$ to intercalators in the presence of DNA (Scheme 2): (I) *intramolecular* photoinduced ET from $Ru(bpy)_3^{2+*}$ bound to DNA electrostatically to intercalators intercalated to the same DNA molecule as $Ru(bpy)_3^{2+}$; (II) *intermolecular* photoinduced ET from ET from $Ru(bpy)_3^{2+*}$ bound to DNA electrostatically to intercalators bound to a different DNA molecule; (III) *intermolecular* photoinduced ET from $Ru(bpy)_3^{2+*}$ bound to DNA electrostatically to free intercalators in solution. These rate constants have been evaluated separately from the decay dynamics of $Ru(bpy)_3^{2+*}$ in the presence of intercalators and DNA and the k_{et} values are summarized in Table 1.

The k_{et} values of *intermolecular* photoinduced ET from $Ru(bpy)_3^{2+*}$ bound to DNA electrostatically to free intercalators in solution (type III in Scheme 2) are virtually the same as those in the absence of DNA. However, the k_{et} values with a large driving force of ET in the presence of DNA, which correspond to the diffusion rate constant, are somewhat smaller than those in its absence because of the smaller diffusion rate constants of *intermolecular* reactions involving two DNA molecules as compared with those involving one DNA molecule (Table 1). In contrast, the k_{et} values of *intermolecular* photoinduced ET from $Ru(bpy)_3^{2+*}$ bound to DNA electrostatically to intercalators bound to a different DNA molecule (type III in Scheme 2) are significantly larger than those of type II in Scheme 2. This is ascribed to the larger driving force of photoinduced ET of intercalated molecules into DNA due to the positive shift of the E^0_{red} values by intercalation. For example, the free energy change of ET from $Ru(bpy)_3^{2+*}$ to 4-MePhen$^+$ in the presence of DNA becomes negative ($\Delta G^\circ_{et} = -0.09$ eV) in contrast with the case in the absence of DNA ($\Delta G^\circ_{et} = +0.04$ eV). In accordance with such a critical change of the ΔG°_{et} value, no transient absorption spectrum due to 4-MePhen$^\bullet$ was observed in the laser flash photolysis experiments of the 4-MePhen$^+$-$Ru(bpy)_3^{2+}$ system in the absence of DNA as shown in Fig. 10 (open circles), whereas the addition of DNA to the 4-MePhen$^+$-$Ru(bpy)_3^{2+}$ system has made it possible to observe a broad transient absorption band around

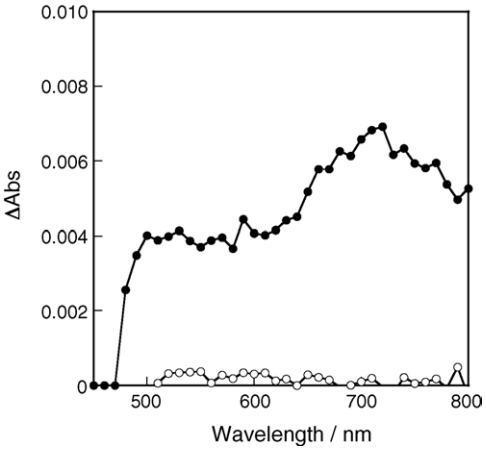

Fig. 10. Transient absorption spectra of an aqueous solution of 4-MePhen$^+$ (1.0×10^{-3} M) and $Ru(bpy)_3^{2+}$ (1.0×10^{-4} M) in the absence of DNA (○) and in the presence (2.0×10^{-3} M) of DNA (●) at 298 K taken at 8 μs after laser excitation at 450 nm.

600–700 nm due to 4-MePhen$^\bullet$ (closed circles in Fig. 10) [44].

As the case of 4-MePhen, no transient absorption spectrum due to QuH$^\bullet$ was observed in the laser flash photolysis experiments of the QuH$^+$-$Ru(bpy)_3^{2+}$ system in the absence of DNA, when the ΔG°_{et} value (+0.05 eV) is positive (endergonic) [17]. However, the addition of DNA to the QuH$^+$-$Ru(bpy)_3^{2+}$ system results in observation of the transient absorption band at 520 nm due to QuH$^\bullet$ [45], when the ΔG°_{et} value (−0.08 eV) becomes negative (exergonic) [17].

The driving force dependence of k_{et} for both type II and type III *intermolecular* photoinduced ET agrees with each other as shown in Fig. 11, where the difference in the driving force between the absence and presence of DNA is taken account [46]. Fitting the data in Fig. 11 with the Marcus equation (Eq. (5)) for both type II and III *intermolecular* photoinduced ET affords the same reorganization energy (0.60 eV) of photoinduced ET in the absence of DNA in Fig. 6.

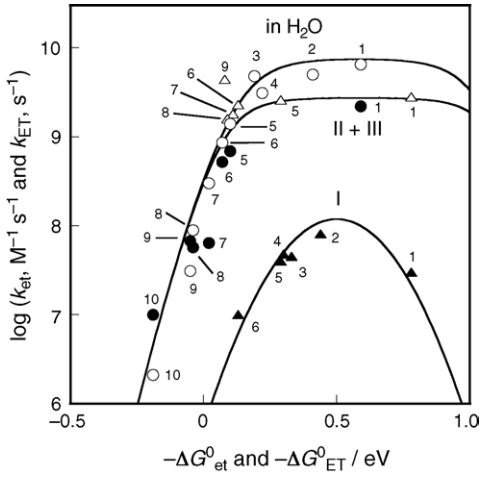

Fig. 11. Marcus plots of log k_{et} vs. $-\Delta G^\circ_{et}$ for intermolecular ET and log k_{et} vs. $-\Delta G^\circ_{ET}$ for intramolecular ET. Numbers refer to intercalators in Table 1. (I)–(III) denote three types of ET in Scheme 2.

The driving force dependence of rate constants of *intramolecular* photoinduced ET (k_{ET}) (type I in Scheme 2) in Fig. 11 (open triangles) can be analyzed using the Marcus equation of non-adiabatic *intramolecular* ET (Eq. (7)),

$$k_{ET} = \left(\frac{4\pi^3}{h^2\lambda k_B T}\right)^{1/2} V^2 \exp\left[\frac{(\Delta G^\circ_{ET} + \lambda)^2}{4\lambda k_B T}\right] \quad (7)$$

where λ is reorganization energy of photoinduced ET, V the coupling matrix element and h the Planck constant [23]. The reasonable fit of the data for the data to a single Marcus curve affords the values of λ = 0.50 eV and $V = 2.0\ cm^{-1}$ (open triangles in Fig. 11). In this case, the k_{ET} value of $AcrH^+$ which has the larger driving force than the λ value is smaller than the values with the smaller driving forces. This indicates that the *intramolecular* photoinduced ET of $AcrH^+$, which is intercalated into DNA, is in the Marcus inverted region. When the driving force is smaller than 0.2 eV, the rates of *intramolecular* photoinduced ET (type I in Scheme 2) become much smaller than those of *intermolecular* photoinduced ET (type II and type III in Scheme 2). In such a case, the emission of $Ru(bpy)_3^{2+*}$ exhibits single-exponential decay (e.g., Fig. 8a).

The small λ value (0.50 eV) for *intramolecular* photoinduced ET (type I in Scheme 2) as compared with the λ value (0.60 eV) for both type II and III *intermolecular* photoinduced ET indicates that electron transfer in DNA requires only small reorganization energy.

4. Conclusions

The effects of DNA on the driving force dependence of photoinduced ET from $Ru(bpy)_3^{2+*}$ bound electrostatically to DNA to intercalators have been clarified. The *intramolecular* pathway of photoinduced ET from $Ru(bpy)_3^{2+*}$ bound electrostatically to DNA to intercalators bound to the same DNA molecule has been distinguished from the *intermolecular* pathway of photoinduced ET of intercalators bound to a different DNA molecule. The k_{et} values of intercalated molecules become much larger than those of free intercalators in solution due to the positive shift in the E^0_{red} values by the intercalation into DNA. Such acceleration effects of DNA on the photoinduced electron-transfer reactions shows sharp contrast with the case of hydride transfer from BNAH to $AcrH^+$ in which the intercalation of $AcrH^+$ into DNA prohibits the reaction due to the steric hindrance of the base pairs toward BNAH (Scheme 1).

Acknowledgements

This work was partially supported by Grants-in-Aid for Scientific Research (No. 13440216) from the Ministry of Education, Culture, Sports, Science and Technology, Japan.

References

[1] (a) J.K. Barton, C.V. Kumar, N.J. Turro, J. Am. Chem. Soc. 108 (1986) 6391;
(b) M.D. Purugganan, C.V. Kumar, N.J. Turro, J.K. Barton, Science 241 (1988) 1645;
(c) E.D.A. Stemp, J.K. Barton, Met. Ions Biol. Syst. 33 (1996) 325;
(d) J.K. Barton, J. Org. Chem. 68 (2003) 6475.
[2] (a) M.R. Arkin, E.D.A. Stemp, R.E. Holmlin, J.K. Barton, A. Hörmann, E.T.C. Olson, P.F. Barbara, Science 273 (1996) 475;
(b) D.B. Hall, R.E. Holmlin, J.K. Barton, Nature 382 (1996) 731.
[3] (a) K.E. Erkkila, D.T. Odom, J.K. Barton, Chem. Rev. 99 (1999) 2777;
(b) C.J. Burrows, J.G. Muller, Chem. Rev. 98 (1998) 1109;
(c) B. Armitage, B. Chem. Rev. 98 (1998) 1171.
[4] (a) R.E. Holmlin, P.J. Dandliker, J.K. Barton, Angew. Chem., Int. Ed. Engl. 36 (1997) 2714;
(b) M.E. Núnez, D.B. Hall, J.K. Barton, Chem. Biol. 6 (1999) 85.
[5] (a) F.D. Lewis, T. Wu, Y. Zhang, R.L. Letsinger, S.R. Greenfiled, M.R. Wasielewski, Science 277 (1997) 673;
(b) F.D. Lewis, R.L. Letsinger, M.R. Wasielewski, Acc. Chem. Res. 34 (2001) 159;
(c) F.D. Lewis, X. Liu, J. Liu, S.E. Miller, R.T. Hayes, M.R. Wasielewski, Nature 406 (2000) 51.
[6] F.D. Lewis, V. Balzani (Eds.), Electron Transfer in Chemistry, 3, Wiley–VCH, Weinheim, 2001, pp. 105–175.
[7] (a) B. Giese, Acc. Chem. Res. 33 (2000) 631;
(b) B. Giese, Annu. Rev. Biochem. 71 (2002) 51;
(c) B. Giese, J. Amaudrut, A.K. Kohler, M. Spormann, S. Wessley, Nature 412 (2001) 318;
(d) E. Meggers, A. Dussy, T. Schäfer, B. Giese, Chem. Eur. J. 6 (2000) 485.
[8] (a) C.J. Murphy, M.R. Arkin, N.D. Ghatlia, S. Bossmann, N.J. Turro, J.K. Barton, Proc. Natl. Acad. Sci. U.S.A. 91 (1994) 5315;
(b) P.J. Dandliker, R.E. Holmlin, J.K. Barton, Science 275 (1997) 1465.
[9] G.B. Schuster, Acc. Chem. Res. 33 (2000) 253.
[10] (a) S. Kanvah, G.B. Schuster, J. Am. Chem. Soc. 124 (2002) 11286;
(b) S.M. Gasper, G.B. Schuster, J. Am. Chem. Soc. 119 (1997) 12762;
(c) P.T. Henderson, D. Jones, G. Hampikian, Y. Kan, G.B. Schuster, Proc. Natl. Acad. Sci. U.S.A. 96 (1999) 8353.
[11] K. Fukui, K. Tanaka, Angew. Chem. Int. Ed. 37 (1998) 158.
[12] (a) A.M. Brun, A. Harriman, J. Am. Chem. Soc. 114 (1992) 3656;
(b) A. Harriman, Angew. Chem., Int. Ed. 38 (1999) 945.
[13] T. Carell, C. Behrens, J. Gierlich, Org. Biomol. Chem. 1 (2003) 2221.
[14] J.J. Storhoff, C.A. Mirkin, Chem. Rev. 99 (1999) 1849.
[15] (a) N.C. Seeman, Nature 421 (2003) 427;
(b) N.C. Seeman, Angew. Chem., Int. Ed. 37 (1998) 3220.
[16] (a) R.F. Anderson, G.A. Wright, Phys. Chem. Chem. Phys. 1 (1999) 4827;
(b) R.F. Anderson, K.B. Patel, W.R. Wilson, J. Chem. Soc., Faraday Trans. 87 (1991) 3739.
[17] M. Nishimine, K. Ohkubo, T. Komori, S. Fukuzumi, A preliminary report, Chem. Commun. (2003) 1886.
[18] (a) A.M. Pyle, J.P. Rehmann, R. Meshroyer, C.V. Kumar, N.J. Turro, J.K. Barton, J. Am. Chem. Soc. 111 (1989) 3051;
(b) C.V. Kumar, J.K. Barton, N.J. Turro, J. Am. Chem. Soc. 107 (1985) 5518.
[19] P. Lincoln, B. Nordén, J. Phys. Chem. B 102 (1998) 9583.
[20] The trigonal ruthenium complexes are preferentially located in the minor groove, although there have been suggestions about the major groove binding as well. See;
(a) I. Greguric, J.R. Aldrich-Wright, J.G. Collins, J. Am. Chem. Soc. 119 (1997) 3621;

(b) E. Tuite, P. Lincoln, B. Nordén, J. Am. Chem. Soc. 119 (1997) 239;
(c) C.M. Dupureur, J.K. Barton, J. Am. Chem. Soc. 116 (1994) 10286;
(d) J.K. Barton, J.M. Goldberg, C.V. Kumar, N.J. Turro, J. Am. Chem. Soc. 108 (1986) 2081.

[21] In contrast to the case of $Ru(bpy)_3^{2+}$ which does not intercalate into DNA base pairs, Δ- and Λ-enantiomers of $Ru(phen)_3^{2+}$ (phen = 1,10-phenathroline) are reported to bind with DNA by quasi-intercalation (indenture of one base pair) [19].

[22] (a) R.A. Marcus, H. Eyrin, Ann. Rev. Phys. Chem. 15 (1964) 155;
(b) R.A. Marcus, Angew. Chem., Int. Ed. Engl. 32 (1993) 1111.

[23] R.A. Marcus, N. Sutin, Biochim. Biophys. Acta 811 (1985) 265.

[24] I. Gould, S. Farid, Acc. Chem. Res. 29 (1996) 522.

[25] R.M.G. Roberts, D. Ostovic, M.M. Kreevoy, Faraday Discuss. Chem. Soc. 74 (1982) 257.

[26] S. Fukuzumi, S. Koumitsu, K. Hironaka, T. Tanaka, J. Am. Chem. Soc. 109 (1987) 305.

[27] (a) S. Fukuzumi, K. Ohkubo, Y. Tokuda, T. Suenobu, J. Am. Chem. Soc. 122 (2000) 4286;
(b) S. Fukuzumi, M. Nishimine, K. Ohkubo, N.V. Tkachenko, H. Lemmetyinen, J. Phys. Chem. B 107 (2003) 12511.

[28] D.D. Perrin, W.L.F. Armarego, D.R. Perrin, Purification of Laboratory Chemicals, 4th ed., Pergamon Press, Elmsford, NY, 1996.

[29] The SHACV method provides a superior approach to directly evaluating the one-electron redox potentials in the presence of a follow-up chemical reaction, relative to the better-known dc and fundamental harmonic ac methods;
(a) A.J. Bard, L.R. Faulkner, Electrochemical Methods Fundamental and Applications, John Wiley and Sons, New York, 2001, p. 368–416, Chapter 10;
(b) T.G. McCord, D.E. Smith, Anal. Chem. 41 (1969) 1423;
(c) A.M. Bond, D.E. Smith, Anal. Chem. 46 (1974) 1946;
(d) M.R. Wasielewski, R. Breslow, J. Am. Chem. Soc. 98 (1976) 4222;
(e) E.M. Arnett, K. Amarnath, N.G. Harvey, J.-P. Cheng, J. Am. Chem. Soc. 112 (1990) 344.

[30] C.K. Mann, K.K. Barnes, Electrochemical Reactions in Nonaqueous Systems, Marcel Dekker, New York, 1990.

[31] M.E. Reichmann, S.A. Rice, C.A. Thomas, P. Doty, J. Am. Chem. Soc. 76 (1954) 3047.

[32] (a) D. Ostovic, R.M.G. Roberts, M.M. Kreevoy, J. Am. Chem. Soc. 105 (1983) 7629;
(b) M.M. Kreevoy, I.-S.H. Lee, J. Am. Chem. Soc. 106 (1984) 2550.

[33] C.-T. Lin, N. Sutin, J. Phys. Chem. 80 (1976) 97.

[34] C. Creutz, N. Sutin, Inorg. Chem. 15 (1976) 496.

[35] R.C. Bock, J.A. Connor, A.R. Gutierrez, T.J. Meyer, D.G. Whitten, B.P. Sullivan, J.K. Nagle, The E_{ox}^{0*} value in acetonitrile was reported to be -0.81 ± 0.07 V (vs. SCE), J. Am. Chem. Soc. 101 (1979) 4815.

[36] In contrast to the case of $Ru(bpy)_3^{2+}$, multi-exponential fluorescence decays of ruthenium complexes which have 1,10-phenanthroline and its related ligands have been observed in the presence of DNA. See;
(a) A. Hergueta-Bravo, M.E. Jiménez-Hernández, F. Montero, E. Oliveros, G. Orellana, J. Phys. Chem. B 106 (2002) 4010;
(b) C. Hiort, P. Lincoln, B. Nordén, J. Am. Chem. Soc. 115 (1993) 3448;
(c) S.A. Tysoe, R.J. Morgan, A.D. Baker, T.C. Strekas, J. Phys. Chem. 97 (1993) 1707.

[37] (a) M. Fujita, A. Ishida, S. Takamuku, S. Fukuzumi, J. Am. Chem. Soc. 118 (1996) 8566;
(b) K. Ohkubo, K. Suga, K. Morikawa, S. Fukuzumi, J. Am. Chem. Soc. 125 (2003) 12850.

[38] G.J. Kavarnos, Fundamentals of Photoinduced Electron Transfer, Wiley–VCH, New York, 1993.

[39] The two-exponential decay is not ascribed to the Δ- and Λ-enanthiomers of $Ru(bpy)_3^{2+}$, since a single exponential decay is observed for other intercalators (see Fig. 8a) and the Δ- and Λ-enanthiomers of $Ru(bpy)_3^{2+}$ are known to afford the identical photodynamics[18].

[40] M. Bixon, M. Jortner, Adv. Chem. Phys. 106 (1999) 35.

[41] (a) J.R. Winkler, H.B. Gray, Chem. Rev. 92 (1992) 369;
(b) H.B. Gray, J.R. Winkler, Quart. Rev. Biophys. 36 (2003) 341.

[42] M.R. Wasielewski, Chem. Rev. 92 (1992) 435.

[43] F.D. Lewis, R.S. Kalgutkar, Y. Wu, X. Liu, J. Liu, R.T. Hayes, S.E. Miller, M.R. Wasielewski, J. Am. Chem. Soc. 122 (2000) 12346.

[44] E.M. Kosower, E.J. Land, A.J. Swallow, The transient absorption band of pyridinyl radical analogs has been reported as λ_{max} = 650–1250 nm, J. Am. Chem. Soc. 94 (1972) 986.

[45] R.F. Cozzens, T.A. Gover, The transient absorption band observed at 520 nm is assigned to QuH, J. Phys. Chem. 74 (1970) 3003.

[46] The back electron transfer processes were not included in the driving force dependence, because the oxidation of DNA with $Ru(bpy)_3^{3+}$ has preculded the accurate determination of the back electron transfer rates.